Energy Metrics Assessment of a Photovoltaic Thermal Air Collector: A Comparison between Flat and Wavy Collector

[1]Prabhakar Jha, [2]Jayanta Deb Mondol, [1,2*]Biplab Das, [3]Rajat Gupta

[1]Department of Mechanical Engineering, NIT Silchar, Assam, 788010, India

2Belfast School of Architecture and the Built Environment, Centre for Sustainable Technology, Ulster University, UK

[3]Department of Mechanical Engineering, NIT Mizoram, Aizwal 796012, India

*Corresponding address: biplab.2kmech@gmail.com; Ph (m):+91-9402168938; Fax: +91-3842224797

Abstract

In this paper, the performances of two different configurations of the PVT air collector (PVTAC) were studied and compared with respect to three energy matrices: energy payback time, electricity production factor and life cycle conversion efficiency. Geometrically, both configurations are similar except one equipped with a flat plate collector (PVTACF) and other with a wavy plate collector (PVTACW). An experimental investigation was performed for both the models, located at Silchar (Latitude: 24.8333° N and Longitude: 92.7789° E) over a period of one year (May 2017 to April 2018). Initially, airflow velocity was varied between 1-3 m/s and ideal airflow velocity (2.5 m/s) was identified. The yearly energetic and exergetic performance was studied and presented. The overall annual energy and exergy of the PVTACW were achieved by 8.2 % and 2.3 % higher than the PVTACF. The energy payback time, electricity production factor, and life cycle conversion efficiency of the PVTACW were also achieved better than the PVTACF. The study provides useful information on the energetic performance and environmental impact of the PVTAC system under North-East Indian climatic conditions.

Keywords: *Photovoltaic thermal air collector; energy matrices; payback time; conversion efficiency; carbon dioxide mitigation*

1. Introduction

Before the technological revolution, human civilization depended completely on non-conventional energy sources to supply energy for most of the human activities such as cooking, transportation, etc. However, in the last 150 years, the need for energy has progressively risen globally [1]. Thus, the novel methods of energy conservation, supply as well as environmental stewardship are highly covetable [2]. Even today, the pursuit of energy-efficient systems continues with physicists and engineers inventing novel technology/techniques and technically efficient systems to solve the situation. The global demand for energy calls for the application of non-conventional energy sources in multitudinous applications [3]. Solar energy is progressed as one such non-conventional energy source and considered as a feasible energy source with enormous potential given the sun shines universally and at the solar belt [4]. Solar energy is primarily harvested using two highly mature technology; solar thermal technology to transform solar energy into thermal energy utilizing solar thermal collector and solar photovoltaic (PV) technology to transform solar energy into electrical energy [5]. A solar thermal collector is one of the most advanced solar technology and is commercially available at a very effective cost [6]. Solar thermal technology is used effectively in domestic, industrial and agricultural applications [7]. The integration of solar thermal collector and PV unit is known as a photovoltaic thermal collector (PVTC) system and can produce both thermal and electrical energy simultaneously [8].

The idea of PVTC technology was conceptualized by Wolf [9] who utilized water as a cooling fluid to cool down the PV module to enhance its electrical efficiency. Following this research, various ground-breaking researches were

conducted across the world to improve the efficacy of PVTC technology. One effective approach to enhance the efficacy of the PVTC system is the integration of a modified absorber plate inside the fluid channel of the collector. Othman et al. [10] implemented a ∇ (del) grooved absorber plate in the flow channel of a PVTAC, and compared its findings with that of the traditional PVTAC. The result revealed that the del grooved absorber plate improved the thermal efficiency of the PVTAC by 30 % as compared to its counterpart. Dimri et al. [11] explored the possibility of improving the thermal efficacy of the PVTAC by utilizing thermoelectric cooler in the air channel of a PVTAC, which eventually enhanced the thermal efficiency by 4.73%, respectively. Fudhoil et al. [12] adopted a theoretical and experimental approach to perform an exergy analysis of a PVTAC with ∇-corrugated absorber plate. The findings of the study revealed that the ∇-corrugated based PVTAC generated theoretical and experimental exergy efficiency of 13.3% and 12.8%. Hussain et al. [13] modified a traditional PVTAC by integrating a honeycomb-shaped absorber plate. The experimental result revealed that the modified PVTAC generated a thermal efficiency of 87 % against 27 % of a traditional PVTAC. The thermal performance of a PVTAC coupled with V corrugated absorber plate was presented by Singh et al. [14] for the range of absorber shape factors. The research communicated that the adopted system has better thermal behavior when the absorber shape factor values lie in the range of 1.3-2. The efficacy of fins in the PVTAC was studied by Bahrehmand et al. [15] where they found that the increase in the number of fins increases the overall efficiency of the system. Mojumder et al. [16] conducted a study to optimize the number of fins for a PVTAC. The study was performed for the range of fin numbers (0-4). The study reported a maximum electrical efficiency of 13.7% at 4 numbers of fins. Slimani et al. [17] carried out a numerical investigation of a finned equipped PVTAC by varying the number of finned rows. The investigation concluded an improvement in electrical and thermal efficiency by 0.3% and 7% when the number of finned rows varied from 6 to 24.

The airflow speed is also a dominant parameter that affects the efficacy of the PVT system. Tiwari et al. [18] analytically investigated the thermal behavior of a PVTAC for the range of airflow speeds (1-8 m/s). The results show that the highest overall thermal efficiency of 30.05% was achieved at the airflow speed of 2 m/s. The energy and exergy efficiency of a PVTAC quipped with a monocrystalline PV module was investigated by Ozakin and Kaya [19] for the range of airflow rates. The study concluded that as the airflow rate changed from 0.05-0.065 kg/s, the energy and exergy efficiency was varied from 64–65.5% and 45-46%.

The energy generation behavior of a PVTAC was also explored by many researchers for a specific metrological condition. One such study was conducted by Agarwal and Tiwari [20] where they explored the energy generation potential of a PVTAC in the metrological condition of New Delhi, India. They found that the system has the potential to generate overall energy and exergy of 1252 kWh and 289.5 kWh. The similar location-dependent study was conducted by Brideau and Collins [21] and Yang et al. [22] in Canada to assess the thermal performance of a PVTAC system whereas Jha et al. [23] assessed the thermal behavior of a PVTAC in the northeastern part of India, which suggested that the PVTAC provides better performance during the noontime. Bagheri and Azimi [24] assessed the power generation capability of a PVTAC for two different climate zones in Iran (Zahedan and Tabriz). It was found that the system has the potential to generate power of 2179.51 kWh and 2007.65 kWh for Zahedan and Tabriz, respectively.

Life cycle assessment (LCA) has been defined as a methodological tool that is widely adopted for analyzing the environmental impacts throughout the life cycle of the product, starting with materials extraction to the manufacturing procedures and at the end with disposal or recycling. The LCA study is performed with the help of three basic energy matrices. These are energy payback time (EPBT), electricity production factor (EPF) and life cycle conversion efficiency (LCCE) [25]. Tripanagnostopoulos et al. [26] performed an LCA of a PVTAC in Patras, Greece. The EPBT from the study has been found

as one year. Raman and Tiwari (2008) conducted an LCA study of a PVTAC in New Delhi, located in the northern part of India. The EPBT, EPF and LCCE were found to be 2.90 years, 0.34 and 0.10, respectively, based on overall heat energy and exergy yield. LCA study of a PVTAC was carried out by Shyam et al. [27] where the EPBT was achieved as 1.1 and 7.7 years based on overall heat energy and exergy yield. Barone et al. [28] numerically assessed the EPBT of a low-cost PVTAC for 8 different climate zones of Europe. Simulation results highlighted the effectiveness of the adopted system, estimating an EPBT in the range of 3.2–4.8 years. Tripathi et al. [29] compared the energy matrices of a concentrated PVTC with two different types of cooling fluid (air and water). The results show that the water-based PVTC has 63.8% lower EPBT and 177.7% higher EPF as compared to the PVTAC. However, the PVTAC has higher LCCE as compared to the water-based PVTC. Recently, Lamnatou et al. [30] carried out an LCA of the building-integrated PVTC system at Ulster University, UK. The study recommended using recycled materials for the storage system in place of primary ones to make the system economical. Jha et al. [31] carried out an extensive review on LCA of a flat plate PVTAC, where they found that the EPBT, EPF and LCCE of a said system were found in the range of 0.8 to 14 years, 0.4 to 22 and 0.10 to 2.86.

Researchers also conducted studies to analyzed the potential of a renewable system to avoid the release of greenhouses gas into the atmosphere. One such study was performed by Bendaoud et al. [32], where they carried out an economical and ecological study of 30kW PV power plant in northern Algeria. The result revealed that the 30 kW PV power plant could earn a reduction of 0.549 tons of carbon dioxide (CO_2) emission during its life span. Rajoria et al. [33] measured the annual reduction of CO_2 for a PVTAC with series and parallel configuration in New Delhi, India. For series and parallel configuration, the CO_2 mitigation per annum was found as 84.52 tCO_2 and 94.05 tCO_2, respectively. Zuhur et al. [34] carried out the CO_2 mitigation analysis of a PVTAC. The findings revealed that the system generated 30W of overall heat energy, which simultaneously resulted in CO_2 mitigation of 0.00007 tons per hour.

Thus, the review showed that the attempts had been made to amplify the thermal behaviour of the PVTAC by modifying the system. But most of the studies are limited to the energetic behaviour of PVTAC. However, less attention has been paid to assess the LCA analysis of a PVTAC. Moreover, the performance of any solar collector is location-dependent and affected by the climatic conditions. As such, no study on a PVTAC has been performed in the composite climate of North Eastern part of India. Further, there is rarely any LCA study has been conducted on a PVTAC equipped with fins or modified absorber plate and compared with the LCA study of a conventional PVTAC. However, when a modification is done over the flat plate, it increases its embodied energy and may not be economical in terms of payback time when compared with the conventional PVTAC (fitted with flat plate). So, in this study, the energetic performance together with LCA analysis of a wavy plate equipped PVTAC versus (aluminum) flat plat equipped PVTAC is performed. The idea behind adopting a wavy plate in this study is mainly due to its easy availability in the Indian market as this is used for house roofing. The wavy plate also has a less impact on the embodied energy because of simpler modification over the flat plate. The present study aimed to experimentally investigate the performance of a PVTAC integrated with a flat plate and wavy plate at Silchar (Latitude: 24.8333° N and Longitude: 92.7789° E), located in the north-eastern part of India. First, an optimum airflow velocity was identified for a PVTAC, and with this optimized airflow velocity, the study was extended to assess the performance of this system.

2. Experimental system

2.1. PVT air collector (PVTAC)

Two models of a PVTAC are fabricated, which are similar in geometric configurations except for the absorber plate. One model of a PVTAC is equipped with a flat absorber plate and named as a photovoltaic thermal air collector with a flat plate (PVTACF) while the other one has a wavy absorber plate and named as photovoltaic thermal air collector with a wavy plate

(PVTACW). The experimental setup consists of a polycrystalline type PV module with a glass-tedlar type configuration. The PV module has an area of 0.745 m^2. The 100 Watt PV module consists of 36 numbers of PV cells. The PV module is placed on the top of an air duct. The rectangular air duct is made of a PVC sheet and a depth of air duct is 0.03 m. The entire setup is placed on a supporting structure made of mild steel. Both the absorber plates are made of an aluminum sheet. The thickness of a used aluminum sheet is 0.001 m. The wavy plate has an amplitude of 0.073 m and a wavelength of 0.006 m. Both the system is properly sealed with putty and rockwool to avoid any leakage of air and heat losses. Both the system are kept inclined at 25° to the horizontal, which is almost equal to the latitude of Silchar. The schematic diagram and a real photograph of the experimental systems are shown in Fig .1(a) and Fig. 1(b). The design parameters used for fabricating the experimental setup are summarized in Table 1(a).

2.2. Instruments used

RTD-PT-100 type temperature sensors were utilized to record the temperature of inlet air, outlet air, ambient air, and PV modules. DT85 type data logger was utilized to display and record the data taken by the temperature sensors. The solar intensity was measured with the help of a Kipp and Zonen type pyranometer. A 24-watt capacity direct current (DC) fan was utilized to supply the forced air into the duct to excerpt the heat energy from the air duct. The airflow velocity was measured by using an anemometer. Other important parameters of the measuring instruments are given in Table 1(b). The positions of the temperature sensors are shown in Fig. 1(a).

3. Thermal modeling of PVTAC

Following quasi-steady-state energy balance, equations for PVTAC are used [35].

3.1. Electrical energy gain

Electrical energy output(E_{annual}) from the PVTAC can be achieved as [36]:

$$E_{ele} = \eta_c \times A \times I(t) \tag{1}$$

where *A* is the PV module area, *I (t)* is the incident solar intensity, η_c is the PV module electrical efficiency (temperature-dependent), which is expressed as [36]:

$$\eta_c = \eta_{ref} \times \left[1 - \beta_{ref} \times (T_m - T_{ref})\right] \tag{2}$$

Where η_{ref}, β_{ref} and T_{ref}, are the PV module efficiency, temperature coefficient of efficiency and temperature at a reference condition. T_m is the PV module temperature.

3.2. Useful heat gain

The rate of heat gain (Q_{hourly}) from a single unit of a PVTAC is the quantity of thermal energy received per second. It can be expressed as [37]:

$$Q_{hourly} = m_a c_a (T_o - T_{fi}) \tag{3}$$

Where m_a, C_a, T_o and T_{fi} are the mass flow rate, specific heat, outlet temperature and inlet temperature of the air.

The daily (Q_{daily}) and monthly $(Q_{monthly})$ heat gain from the PVTAC can be obtained as [38]:

$$Q_{daily} = \sum_{i=1}^{m} Q_{hourlyi} \tag{4}$$

$$Q_{monthly} = \sum_{i=1}^{n} Q_{dailyi} \tag{5}$$

The overall heat energy (Q_{ovther}) gain can be expressed as [36]:

$$Q_{ovther} = \sum_{i=1}^{12} Q_{monthlyi} + \frac{E_{annual}}{C_f} \tag{6}$$

Where C_f is equal to 0.38, which is known as a conversion coefficient for coal-based thermal power plant, *m* and *n* represent a number of sunshine hours and days, respectively, in which the experiment was performed.

Thermal efficiency can be expressed as [20]:

$$\eta_{ther} = \frac{Q_{hourly}}{b \times L \times I(t)} \tag{7}$$

Where *b* and *L* are the width and length of the collector.

Whereas, the overall energy efficiency can be expressed as [18]:

$$\eta_{overall} = \frac{\sum \left[\eta_c I(t) bL + Q_{hourly}\right]}{\sum I(t) bL} \tag{8}$$

3.3. Useful exergy gain

The analysis of exergy uses the principles of energy and mass conservation coupled with the second law of thermodynamics [35].

Hourly exergy can be estimated as [36]:

$$E_{ex} = Q_{hourly}\left[1 - \frac{T_a + 273}{T_o + 273}\right] \tag{9}$$

Where T_a is the ambient temperature.

The electrical energy obtained from a PVTAC is a subsequent form of exergy and so, the overall exergy output (E_{ovex}) can be described as the summation of the thermal exergy output (E_{ex}) and electrical energy output (E_{ele}). This is expressed as [39]:

$$E_{ovex} = \sum E_{ex} + \sum E_{el} \tag{10}$$

4. Life cycle energy metrics

4.1. Embodied energy (E_{in})

The embodied energy is defined as "the quantity of the energy spent to prepare the materials, used in the fabrication of the system along with its components" [39]. The embodied energy of several components used in the experiments is presented in Table 2.

4.2. Energy payback time (EPBT)

The EPBT is the number of years needed for the system to recover the energy spent in the manufacturing and fabrication of the system along with the components. It is expressed as [39]:

$$EPBT = \frac{E_{in}}{E_{out}} \text{ in years} \tag{11}$$

E_{out} represents the overall energy/exergy gain obtained from equations (6) and (10) and E_{in} is the value of embodied energy.

4.3 Electricity production factor (EPF)

The EPF is a factor, which depicts the performance of the PVTAC by relating the input energy to the overall output energy or exergy. The EPF is also known as reciprocal of EPBT [40].
EPF can be evaluated on two bases, as it is a function of time [40]:

- annual basis
- life time basis

The EPF on the annual and life time basis is expressed as [40]:

$$X_a(t) = \frac{E_{out}}{E_{in}} \text{ or} \tag{12}$$

$$X_L(t) = \frac{E_{out} \times T}{E_{in}} \tag{13}$$

Where, X_a and X_L are the EPF as an annual and life time basis, respectively. T is known as the life span of the PVTAC.

4.4. Life cycle conversion efficiency (LCCE)

The productivity of the PVTAC, in terms of overall energy and exergy with respect to the incident sun intensity during its life span is called as LCCE ($\emptyset(t)$). This is expressed as [41]:

$$\phi(t) = \frac{(E_{out} \times T) - E_{in}}{E_{out}} = \frac{E_{out}}{E_{in}}\left[1 - \frac{E_{in}}{E_{out} \times T}\right] \tag{14}$$

$$= \eta\left[1 - \frac{1}{X(t) \times T}\right] \tag{15}$$

where the value of η is 0.14 for the present study.

4.5. Environmental cost analysis

In this study, the enviro-economic assessment is done to assess the cost of CO_2 mitigation. This knowledge of CO_2 mitigation and its corresponding cost promotes the idea of using renewable energy as a clean and carbon-free resource. For electricity generation from coal, the equivalent production of CO_2 is 0.98 kg CO_2/kWh, approximately. However, for Indian condition, this value is refigured to 1.58 kg CO_2/kWh, after considering the distribution and transmission losses as 40% and the appliances losses as 20%. Therefore, the annual reduction of CO_2 emission can be expressed as [41]:

CO_2 mitigation per annum= $E_{out} \times 1.58$ (16)

If the cost of CO_2 reduction in the international market is traded as €20/ton of CO_2 mitigation.

Therefore, the carbon credit earned per annum = CO_2 mitigation per annum× €20/ton of CO_2mitigation [42]

Where 1€ ≈ Rs 78.8 as of June 2018. (17)

5. Uncertainty analysis

Uncertainty analysis of the instruments used in the experimental investigation must be calculated to present the accurate findings of the research. In this study, the uncertainty analysis is carried out with the help of eq. (18), which suggest that the uncertainty of the dependent variable (r) is a function of the uncertainty of the independent variables ($v_1, v_2, \ldots, v_n$), which is expressed as [43]:

$$e_r = \sqrt{\left(\frac{\partial r}{\partial v_1} e_1\right)^2 + \left(\frac{\partial r}{\partial v_2} e_2\right)^2 + \cdots + \left(\frac{\partial r}{\partial v_n} e_n\right)^2} \quad (18)$$

Where e_r represents the uncertainty in the experimental results and the partial derivative $\frac{\partial r}{\partial v_1}$ represents the sensitivity of the experimental result to a single variable.

Table 1 (b) represents the experimental uncertainty of the measuring instruments used in the experimental investigation. Based on these values, the total experimental uncertainty is calculated as:

$e_r = \sqrt{(1.41)^2 + (0.14)^2 + (0.5)^2}$ = ± 1.5025

The total experimental uncertainty is achieved less than 5%, which indicates that the measuring devices gave readings as per the acceptable limit.

6. Results and discussion

The experimental analysis of the PVTACF and PVTACW was carried out under North East Indian climatic conditions. The experimental study was performed between 9.00 hr to 16:00 hr of the day from May 2017 to April 2018 under different weather conditions of Silchar, India except for rainy days. Results indicated that December and March represented the month with the highest and lowest energetic performance annually. So, to depict the hourly and monthly variation of various parameters and outputs of the PVTACF, and PVTCAW, the 24th December, 2017 and 20th March, 2018 have been chosen. Table 3 summarizes the measured parameters during these two days. Similarly, data are recorded over the years and their corresponding energetic and exergetic outputs were calculated for PVTACF and PVTACW followed by the LCA. In addition, the efficiency of the PV module, and its variation with respect to the operating temperature was also measured. At first, the airflow velocity was optimized, and then the optimized airflow velocity was used to carry out the yearly investigation. For this purpose, the airflow velocity was selected within the range between 1and 3.5 m/s.

6.1. Solar intensity and ambient temperature

The hourly average solar intensity and ambient temperature during the experimental run of the year are summerize in Table 4(a) and 4 (b). The highest and lowest average solar intensity and ambient temperatures were detected for June and December, respectively (see Tables 4a and 4b). The month of March has a moderate yield of solar intensity coupled with less number of rainy days recorded than the other months. This makes March as one of the important months through the year from an energy

point of view. The hourly dissimilarity of solar intensity for the 24th December and 20th March is shown in Fig. 2. For the 24th December and 20th March, the average value of the solar intensity was found to be 373.17 and 531.62W/m^2, respectively.

6.2. Airflow velocity

The maximum efficiency of a specific PVTAC system is observed for an ideal range of air velocity [16,18]. Thus, in this study, the airflow velocity was varied in the range of 1 to 3.5 m/s to evaluate the thermal performance. Fig.3 indicates that for both the systems the overall energy efficiency rises sharply with the increase in airflow velocity due to the rise in heat extraction rate but drops when the air velocity is greater than 2.5 m/s because of lower heat accumulation time of air and increase in leakage losses. This trend is in order with the study reported by Singh et al. [44]. This optimum value (2.5 m/s) of airflow velocity was used to analyze the annual performance of the systems.

6.3. Hourly temperature variation

Hourly temperature variations of the PV module and outlet air are shown in Figs.4 (a & b) for the 24th December and 20th March. The variation of PV module temperature and outlet air temperature with respect to solar intensity for both systems is similar to other studies performed on PVTAC [20, 23] where the maximum temperature is achieved at noon. The module temperature of PVTACW is lower than that of PVTACF due to the higher heat extraction rate from the module. This is because the wavy plate has better heat exchanging surface than a flat plate. This advantage of PVTACW over PVTACF resulted in a higher outlet temperature. The average module temperature of PVTACW for the test day in December and March was observed as 33.3°C and 46.8 °C, respectively as compared to 34.6°C and 48.1°C of PVTACF. The average outlet temperature of PVTACW was observed as 27.9°C and 37.4°C as compared to 26.6 °C and 36.2°C of PVTACF.

6.4. Hourly heat energy, exergy and electrical energy gain

The hourly heat energy and exergy gain for the 24th December and 20th March of the PVTACW were achieved higher than the PVTACF due to efficient heat extraction by the wavy surface as shown in Fig.5 (a &b). The reason for efficient heat extraction by the wavy plate surface is because of better surface contact with flowing air. For the entire day of the 24th December and 20th March, the total heat energy gain achieved from the PVTACW was 491. 55 Wh and 765.26 Wh as compared to 372.48 Wh and 648.77 Wh of the PVTACF. Similarly, for the 24th December and 20th March, the total exergy gain achieved from the PVTACW was 12.09 Wh and 25.80 Wh as compared to 7.59 Wh and 19.17 Wh of the PVTACF. The electrical energy received from the PVTACW for the 24th December and 20th March was 0.69 % and 0.74 % higher than PVTACF as shown in Fig.5(c). The reason for the higher electrical energy of the PVTACW over the PVTACF can be understood from Fig.6, where it is seen that the electrical efficiency amplified with the reduction in the module temperature and at any given instant of time, the PVTACW has lower module temperature than the PVTACF and hence higher electrical efficiency.

6.5. Overall energy and exergy gain

The monthly heat energy and electrical energy gain, over the year, are shown in Fig.7 (a&b). The highest value of the monthly heat and electrical energy gain was found in March. The PVTACW has achieved 19.12 % and 0.72 % higher heat and electrical energy than the PVTACF. The reason for better heat and the electrical energy generation in March is because of the lower number of rainy days than other months for this specific location of North-East, India. The lowest energy generation was achieved in December due to low incident solar intensity, where the PVTACW has achieved 34% and 0.67 % higher heat and electrical energy than the PVTACF. The annual heat energy and electrical energy gain for PVTACW were achieved

21.2 % and 0.73 % higher than the PVTACF, respectively as shown in Fig.7 (a& b). The overall heat energy and exergy gain were calculated using Eqs. (6) and (10) and the results are shown in Fig. 8 (a & b). The overall calculated energy and exergy gain of PVTACW was achieved by 8.2 % and 2.3 % higher, respectively than PVTACF.

6.6. Mitigation of CO_2 emission

The monthly CO_2 mitigation on the basis of heat energy and exergy yield for the PVTACW and PVTACF was also estimated (Fig.9). Both the systems have achieved the highest and lowest value of CO_2 mitigation in March and December, respectively. PVTACW has yielded 7.7 % and 2.3 % higher CO_2 mitigation on the basis of heat energy and exergy than the PVTACF in March, whereas this percentage enhancement was achieved as 11.4 % and 2.1 % in December.

The CO_2 mitigation per annum on energy and exergy basis was achieved as 0.831 tCO_{2e} and 0.198 $tCO_{2e,}$ respectively for PVTACW as compared to 0.768 tCO_{2e} and 0.193 tCO_{2e} of the PVTACF (Fig. 9). This CO_2 mitigation per annum can lead to an environmental cost reduction of €16.6 (Rs. 1310) and €3.9 (Rs.311) on the basis of heat energy and exergy for the PVTACW as compared to €15.5 (Rs. 1210) and €3.7 (Rs.304.5), respectively for the PVTACF. This cost reduction can lead to a better economical aspect considering the life span of the PVTAC.

6.7. EPBT, EPF and LCCE

The overall energetic performance of a PVTAC can be evaluated with the help of three energy matrices (EPBT, EPF and LCCE), which suggests the viability of any system. The EPBT, EPF and LCCE of the PVTACW and PVTACF were calculated using Eqs. (11)-(15) for Silchar, India. The EPBT for the PVTACW was estimated as 1.9 years and 8.2 years on the basis of heat energy and exergy yield as compared to 2.1 years and 8.3 years of the PVTACF. The EPF for the PVTACW was achieved as 0.50 and 0.12 on the basis of heat energy and exergy as compared to 0.47 and 0.11 of the PVTACF, respectively. Again, it is discussed that the EPF and LCCE are a function of time. So, both these parameters were also evaluated by considering the life span of 10, 20 and 30 years on the basis of heat energy and exergy. Table 5 summarizes the calculated values of EPF and LCCE for the said life span of both the PVTAC system. It can be seen that the upsurge in the life span of the systems simultaneously results in the enhancement of EPF and LCCE. Similarly, results were reported by Raman and Tiwari [41]. For the life span of 30 years, the EPF of the PVTACW, on the basis of heat energy and exergy was achieved 7 % and 2.8 % higher than the PVTACF, respectively, while the LCCE was achieved 0.76 % and 1% higher. The discussion suggests the PVTACW has achieved a better value of energy matrices than the PVTACF, even though it has higher embodied energy. This is because the PVTACW has generated sufficient overall heat energy and exergy that outperformed the factor of high embodied energy and resulted in a better energy matrices as compared to its counterpart.

7. Conclusion

Performance assessment of a photovoltaic thermal air collector with a flat (PVTACF) and wavy plate (PVTACW) has been performed using three energy matrices: energy payback time (EPBT), electricity production factor (EPF) and life cycle conversion efficiency (LCCE) under North East Indian climatic condition. The following conclusions have been drawn from the experimental results:

- The highest overall energy gain and exergy gain were obtained in March because of less number of rainy days than the other months, whereas the lowest value has been found in December because of low solar intensity for both the systems.

- The overall annual energy and exergy gains for the PVTACW were achieved 8.2 % and 2.3 % higher, respectively than the PVTACF.
- The EPBT for the PVTACW was estimated as 1.9 years and 8.2 years on the basis of energy and exergy yield against 2.1 years and 8.3 years of the PVTACF.
- The EPF for the PVTACW was calculated as 0.50 and 0.12 on the basis of energy and exergy gain against 0.47 and 0.11 for the PVTACF, respectively.
- The EPF and LCCE increase with the increase in the life span of the systems and has the highest value for the PVTACW than the PVTACF.
- The CO_2 mitigation per annum from the PVTACW was achieved 8.2 % (energy basis) and 2.6 % (exergy basis) higher than the PVTACF.

So, with the above conclusions, it can be said that the PVTAC, when integrated with a wavy plate, offers the best energetic performance and has less payback time over the PVTAC with a flat plate even though it has high embodied energy.

It can be seen that the EPBT achieved from the present study for the PVTAC with a flat plate for the location of Silchar (Northeastern part of India) is different from the similar study conducted in the northern [38] and western part of India [41]. This shows that the different zones of India have different payback times for the same conventional type PVTAC (fitted with flat plate). It can also be concluded from this study that the values of the energy matrices are location-dependent and varies with respect to the climatic conditions. Thus, to estimate the environmental impact and energetic performance of the system accurately, it is recommended that a system-specific experimental performance data is required for a local climatic condition.

Nomenclature

PV	photovoltaic	T_m	module temperature (K)
PVTC	photovoltaic thermal collector	T_{ref}	reference temperature (K)
PVTAC	photovoltaic thermal air collector	T_o	air outlet temperature (K)
PVTACF	photovoltaic thermal air collector with flat plate	T_{fi}	air inlet temperature (K)
		T_a	ambient temperature (K)
PVTACW	photovoltaic thermal air collector with wavy plate	T	life span (years)
		C_f	conversion coefficient
LCA	Life cycle assessment	E_{ele}	electrical energy gain, hourly (W)
EPBT	energy payback time (years)	E_{annual}	electrical energy gain, annually (Wh)
EPF	electricity production factor	Q_{hourly}	heat gain, hourly (W)
LCCE	life cycle conversion efficiency	Q_{daily}	heat gain, daily (Wh)
DC	direct current	$Q_{monthly}$	heat gain, monthly (Wh)
t	tonne	Q_{ovther}	overall heat energy gain (kWh)
A	area of a module (m^2)	E_{ex}	exergy gain, hourly (W)
b	width of the collector (m)	E_{ovex}	overall exergy gain (kWh)
L	length of the collector (m)	E_{in}	embodied energy (kWh)
I(t)	intensity of sun (W/m^2)	E_{out}	overall energy/exergy gain (kWh)
C_a	air specific heat (J/kg-K)	Rs.	rupees
m_a	flow rate of air (kg/s)	hr	hour

Greek letters

$\emptyset$ (t)	life cycle conversion efficiency
X_a	electricity production factor
β_{ref}	temperature coefficient of efficiency (1/K)
η_c	module electrical efficiency (%)
η_{ther}	thermal efficiency (%)
$\eta_{overall}$	overall efficiency (%)
η_{ref}	efficiency of PV module at standard tests condition (%)

References

[1] Buker, M.S., Riffat, S.B., 2015. Building integrated solar thermal collectors – a review. Renewable and Sustainable Energy Reviews 51, 327–346.

[2] Li, C., 2019. Economic and performance evaluation of grid-connected residential solar photovoltaic systems in Northwest China. Energy Sources, Part A: Recovery, Utilization, and Environmental Effects, 1–17.

[3] Das, D., Kalita, P., Roy, O., 2018. Flat plate hybrid photovoltaic- thermal (PV/T) system: A review on design and development. Renewable and Sustainable Energy Reviews 84,111–130.

[4] Abdalla, M., Abuquba, H., 2019. Natural cooling of two axis tracking photovoltaic module. Energy Sources, Part A: Recovery, Utilization, and Environmental Effects,1–16.

[5] Jia, Y., Alva, G., Fang, G., 2019. Development and applications of photovoltaic–thermal systems: A review. Renewable and Sustainable Energy Reviews 102, 249–265.

[6] Das, B., Mondol, J.D., Debnath, S., Pugsley, A., Smyth, M., Zacharopoulos, A., 2020. Effect of the absorber surface roughness on the performance of a solar air collector: an experimental investigation. Renewable Energy 152, 567–572.

[7] Gupta, A., Das, B., Mondol, J.D., 2020. Experimental and theoretical performance analysis of a hybrid photovoltaic-thermal (PVT) solar air dryer for green chilis, International Journal of Ambient Energy,1–31.

[8] Slimani, M.E.A., Amirat, M., Kurucz, I., Bahria, S., Hamidat, A., Chaouch, W.B., 2017. A detailed thermal-electrical model of three photovoltaic/thermal (PV/T) hybrid air collectors and photovoltaic (PV) module: Comparative study under Algiers climatic conditions. Energy Conversion and Management 133,458–476.

[9] Wolf, M.,1976. Performance analyses of combined heating and photovoltaic power systems for residences. Energy Conversion 116, 79–90.

[10] Othman, M.Y.H., Ruslan, H., Sopian, K., Jin, G.L., 2009. Performance study of photovoltaic-thermal (PV/T) solar collector with del-grooved absorber plate. Sains Malaysiana 38, 537–541.

[11] Dimri, N., Tiwari, A., Tiwari, G.N., 2017. Thermal modelling of semitransparent photovoltaic thermal (PVT) with thermoelectric cooler (TEC) collector. Energy Conversion and Management 146, 68–77.

[12] Fudholi, A., Zohria, M., Rukmana, N.S.B., Nazria, N.S., Mustapha, M., Yen, C.H., Mohammad, M., Sopian, K., 2019. Exergy and sustainability index of photovoltaic thermal (PVT) air collector: a theoretical and experimental study. Renewable and Sustainable Energy Review 100, 44–51.

[13] Hussain, F., Othman, M.Y.H., Yatim, B., Ruslan, H., Sopian, K., Anuar, Z., Khairuddin, S., 2015. An improved design of photovoltaic/thermal solar collector. Solar Energy 122, 885–891.

[14] Singh, H.P., Jain, A., Singh, A., Arora, S., 2019. Influence of absorber plate shape factor and mass flow rate on the performance of the PVT system. Applied Thermal Engineering 156, 692–701.

[15] Bahrehmand, D. Ameri, M., Gholampour, M., 2015. Energy and exergy analysis of different solar air collector systems with forced convection. Renewable Energy 83, 1119–1130.

[16] Mojumder, J.C., Chong, W.T., Ong H.W., Leong, K.Y., Mamoon, A.A., 2016. An experimental investigation on performance analysis of air type photovoltaic thermal collector system integrated with cooling fins design. Energy and Buildings 130, 272–285.

[17] Slimani, M.E.A., Sellami, R., Amirat, M., 2019. Study of hybrid photovoltaic/thermal collector provided with finned metal plates: A numerical investigation under real operating conditions. International Conference on Advanced Electrical Engineering, 1–6.

[18] Tiwari, A., Sodha, M.S., Chandra, A., Joshi, J.C., 2006. Performance evaluation of photovoltaic thermal solar air collector for composite climate of India. Solar Energy Materials & Solar Cells 90, 175–189.

[19] Ozakin, A.N., Kaya, F., 2019. Effect on the exergy of the PVT system of fins added to an air-cooled channel: A study on temperature and air velocity with ANSYS Fluent. Solar energy 184, 561–569.

[20] Agrawal, S., Tiwari, G.N., 2012. Exergoeconomic analysis of glazed hybrid photovoltaic thermal module air collector. Solar Energy 86, 2826–2838.

[21] Brideau, S.A., Collins, M.R., 2014. Development and validation of a hybrid PV/Thermal air-based collector model with impinging jets. Sol. Energy 102, 234–246.

[22] Yang, T., Athienitis, A.K., 2015. Experimental investigation of a two-inlet air-based building integrated photovoltaic/thermal (BIPV/T) system. Applied Energy 159, 70–79.

[23] Jha, P., Das, B., Rajat, G., 2019. Energy and exergy analysis of photovoltaic thermal air collector under the climatic condition of North Eastern India. Energy Procedia 158, 1161–1167.

[24] Bagheri, H., Azimi, A., 2020. Thermodynamic analysis of a CCHP system for a building using solar collectors and PV panels in two different climate zones in Iran. Energy Sources, Part A: Recovery, Utilization, and Environmental Effects, 1–20.

[25] Brummelen, M., Engelenburg, B., Nieuwlaar, E.,1994. Methodology for the Life Cycle Assessment of Energy Technologies, Utrecht: Department of Science, Technology and Society of the Utrecht University.

[26] Tripanagnostopoulos, Y., Souliotis, M., Battisti, R., Corrado, A., 2006. Performance, cost and life-cycle assessment study of hybrid pvt/air solar systems. Progress in Photovoltaics: Research and Applications 14, 65–76.

[27] Shyam, Tiwari, G.N., 2016. Analysis of series connected photovoltaic thermal air collectors partially covered by semitransparent photovoltaic module. Solar Energy 137, 452–462.

[28] Barone, G., Buonomano, A., Forzano, C., Palombo, A., Panagopoulos, O., 2019. Experimentation, modelling and applications of a novel low-cost air-based photovoltaic thermal collector prototype. Energy Conversion and Management 195, 1079–1097.

[29] Tripathi, R., Tiwari, G.N., 2019. Energy matrices, life cycle cost, carbon mitigation and credits of open-loop N concentrated photovoltaic thermal (CPVT) collector at cold climate in India: A comparative study. Solar Energy 186, 347–359.

[30] Lamnatou, C., Smyth, M., Chemisana, D., 2019. Building-Integrated Photovoltaic/Thermal (BIPVT): LCA of a façade-integrated prototype and issues about human health, ecosystems, resources. Science of the Total Environment 660, 1576–1592.

[31] Jha, P., Das, B., Rezaie. B., 2019. Significant factors for enhancing the life cycle assessment of photovoltaic thermal air collector. Energy Equipment and Systems 7, 175–197.

[32] Bendaoud, B., Malek, A., Loukarfi, L., Maammeur. H., 2020. Conceptual study of photovoltaic power plant connected to the urban electrical network in northern Algeria. Energy Sources, Part A: Recovery, Utilization, and Environmental Effects, 1–20.

[33] Rajoria, C.S., Agrawal, S., Tiwari, G.N., 2013. Exergetic and enviroeconomic analysis of novel hybrid PVT array. Solar Energy 88,110–119.

[34] Zuhur, S., Ceylan, I., Ergun, A., 2019. Energy, exergy and environmental impact analysis of concentrated PV/cooling system in Turkey. Solar Energy 180, 567–574.

[35] Jha, P., Das, B., Gupta, R., 2019. An experimental study of a photovoltaic thermal air collector (PVTAC): A comparison of a flat and wavy collector, Applied Thermal Engineering 163, 114344.

[36] Kamthania, D., Tiwari, G.N., 2014. Energy metrics analysis of semi-transparent hybrid PVT double pass facade considering various silicon and non-silicon based PV module Hyphen hyphen is accepted. Solar Energy 100, 124–140.

[37] Pathak, P.K., Chandra, P., Raj. G., 2019. Comparative analysis of modified and convectional dual purpose solar collector: Energy and exergy analysis, Energy Sources, Part A: Recovery, Utilization, and Environmental Effects,1–17.

[38] Tiwari, A., Barnwal, P., Sandhu, G.S., Sodha, M.S., 2009. Energy metrics analysis of hybrid photovoltaic (PV) modules. Applied Energy 86, 2615–2625.

[39] Agrawal, S., Tiwari G.N., 2013. Enviroeconomic analysis and energy matrices of glazed hybrid photovoltaic thermal module air collector. Solar Energy 92, 139–146.

[40] Rajoria, C.S., Agrawal, S., Dash, A.K., Tiwari, G.N., Sodha, M.S., 2016. A newer approach on cash flow diagram to investigate the effect of energy payback time and earned carbon credits on life cycle cost of different photovoltaic thermal array systems. Solar Energy 124, 254–267.

[41] Raman, V., Tiwari, G. N., Pandey, H. D., 2008. Life cycle cost analysis of a hybrid photovoltaic-thermal water and air collector: A comparison study. International Journal of Low-Carbon Technologies 3,173–190.

[42] Agrawal. S., Tiwari, G.N., 2015. Performance analysis in terms of carbon credit earned on annualized uniform cost of glazed hybrid photovoltaic thermal air collector. Solar Energy 115, 329–340.

[43] Al-Waeli, A. H., Sopian, K., Chaichan, M.T., Kazem, H. A., Hasan, H. A., Al-Shamani, A. N., 2017. An experimental investigation of SiC nanofluid as a base-fluid for a photovoltaic thermal PV/T system. Energy Conversion and Management 142, 547-558.

[44] Singh, B.S.S, Yen, C.H., Zaidi, S.H., Sopian, K., 2018. Enhanced performance of concentrating photovoltaic thermal air collector with fresnel lens and compound parabolic concentrator. Journal of Advanced Research in Fluid Mechanics and Thermal Sciences 47, 16-24.

Table 1(a). Design parameters for PVTACF and PVTACW.

Design Parameters	**Values**
A	0.745 m^2
L	1.1 m
b	0.678 m
m_a	0.0128 kg/s
C_a	1005 J/kg K
η_{ref}	0.14
β_{ref}	0.0045/K

Table 1(b). Details of instruments used for an investigation.

Sr. No.	Instruments	Parameters	Operating range	Uncertainty (%)
1.	Pyranometer	Solar intensity	0 - 4000 W/m^2	± 1.41
2	Anemometer	Airflow velocity	0 - 25m/s	±0.14
3	Temperature Sensor (RTD-PT-100 type)	Temperature of inlet air, outlet air, ambient air and PV module	-200 to 500 °C	±0.5

Table 2. Break down of the embodied energy for the components used in the PVTACF and PVTACW.

Sr. No.	Component	Quantity		Energy density (kWh/Kg)	Total embodied energy (kWh)	
		PVTACF	**PVTACW**		**PVTACF**	**PVTACW**
1.	Mild steel support structure	11.5 kg	11.5 kg	8.89	97.79	97.79
2.	PV module	0.745 m^2	0.745 m^2	980 kWh/m^2	730.1	730.1
3.	PVC Sheet	2.8 kg	2.8 kg	25.64	71.79	71.79
4.	Alumnium sheet	1.52kg	1.75 kg	55.28	84.02	96.74
5.	Paint	0.5 kg	0.52 kg	25.11	12.55	13.05
6.	DC fan					
	(i) Alumunium	0.38 kg	0.38 kg	55.28	21.00	21.00
	(ii) Plastic	0.125 kg	0.125 kg	19.44	2.43	2.43
	(iii) Iron	0.22 kg	0.22 kg	8.89	1.95	1.95
	(iv) Copper wire	0.05 kg	0.05 kg	19.61	0.98	0.98
				Total	**1022.61**	**1035.83**

Table 3. Measured parameters for the 24th December, 2017 and March 20th March, 2018.

Time	Ambient air temp. (°C)	Inlet air temp. (°C)	PV module temp. (°C)		Outlet air temp. (°C)	
24th December, 2017			**PVTACF**	**PVTACW**	**PVTACF**	**PVTACW**
9:00	17.1	18.4	23	22.3	20.7	21.3
10:00	19.9	21.8	28.8	27.2	24.7	25.8
11:00	21.4	23.3	34.8	33.7	26.8	29
12:00	22.1	25	45.3	43	30.2	31.7
13:00	22.5	25.4	44.4	42.5	30.1	31.4
14:00	22.9	25.7	43.3	42.1	30.2	31.1
15:00	22.7	24.4	31	30	28.4	29.5
16:00	20.4	20.7	26.8	25.8	22.4	23.5
20th March, 2018						
9:00	22.7	25.3	33.9	33.1	31.3	32.1
10:00	24.1	26.5	45.1	43.5	32.6	33.5
11:00	25.9	28	51.8	49.7	34.9	37
12:00	28.6	32.1	59.3	57.1	40.2	41.8
13:00	30.1	32.6	57.1	55.4	40.1	41.3
14:00	30.1	32.7	53.7	52.8	39.4	40.3
15:00	29.5	31.8	48	47.3	38	39.2
16:00	29	31	36.6	36	33.7	34.6

Table 4 (a). Average monthly solar intensity during the experimental run of the year.

Months ↓	**Average solar intensity (W/m^2)**							
Time (Hour) →	09:00	10:00	11:00	12:00	13:00	14:00	15:00	16:00
May, 2017	591	701.7	765.8	811.8	803.4	762.9	515	324.8
June, 2017	599.2	733.7	780.8	854.4	812.8	771.9	526	339.8
July, 2017	572.1	697.8	713.8	804.4	718.8	710.9	445	275.8
August, 2017	520	602.9	665.8	735.4	702	632	410	243.8
September, 2017	510.6	597.7	661.8	720.4	676.8	612.7	390	221.7
October, 2017	399.9	490	567.8	664.4	623.5	520.3	370.9	200
November, 2017	269.9	376.3	496.8	521.4	507.5	451.3	319.9	187
December, 2017	237.2	331.2	449.9	498	475.2	413.2	309.3	163.2
January, 2018	240.3	402.5	513.8	590.6	534	470	358	179
February, 2018	246.8	424.5	531.4	625.4	562.6	487.7	387	181.3
March, 2018	470.1	521.3	617.9	710	679.2	591.9	375.3	190
April, 2018	556.6	580.7	679.8	750.4	741.8	656.9	433	251.8

Table 4 (b). Average monthly ambient temperature during the experimental of the year.

Months ↓	**Average Ambient temperature (°C)**							
Time (Hour) →	09:00	10:00	11:00	12:00	13:00	14:00	15:00	16:00
May, 2017	29.1	29.3	31.1	32.7	33.9	33.6	33.2	33.1
June, 2017	29.7	30.8	32.6	33.7	35	34.7	34.4	34.2
July, 2017	27.7	28.8	30.6	31.7	33	32.7	32.4	31.9
August, 2017	24.9	26	27.7	29.3	31.8	31.6	30.9	29.8
September, 2017	25.7	25.9	27.3	28.9	30.6	30.2	29.8	29.7
October, 2017	22.3	22.9	24.4	26.9	28.5	28.3	28.2	28
November, 2017	17.5	20.1	21.6	23.5	26.5	26.5	25.9	24.9
December, 2017	16.5	19.5	20.9	21.6	22.3	22.2	21.9	19.8
January, 2018	17	21.7	23.7	25.7	28.3	27.9	27.1	26.4
February, 2018	20.6	21.2	23.8	26	28.3	28	27.7	27
March, 2018	22	23.8	26.1	27.7	29.8	29.7	28.9	28.4
April, 2018	26.1	26.8	28.4	29.9	32	31.9	31.2	30.6

Table 5. EPF and LCCE for the life span of 10, 20 and 30 years on the basis of heat energy and exergy.

Life span (years)	**heat energy**				**exergy**			
	EPF		**LCCE**		**EPF**		**LCCE**	
	PVTACF	**PVTACW**	**PVTACF**	**PVTACW**	**PVTACF**	**PVTACW**	**PVTACF**	**PVTACW**
10	4.7	5.0	0.110	0.112	1.1	1.2	0.022	0.024
20	9.5	10.1	0.125	0.126	2.3	2.4	0.081	0.082
30	14.2	15.2	0.130	0.131	3.5	3.6	0.100	0.101

Lists of figures

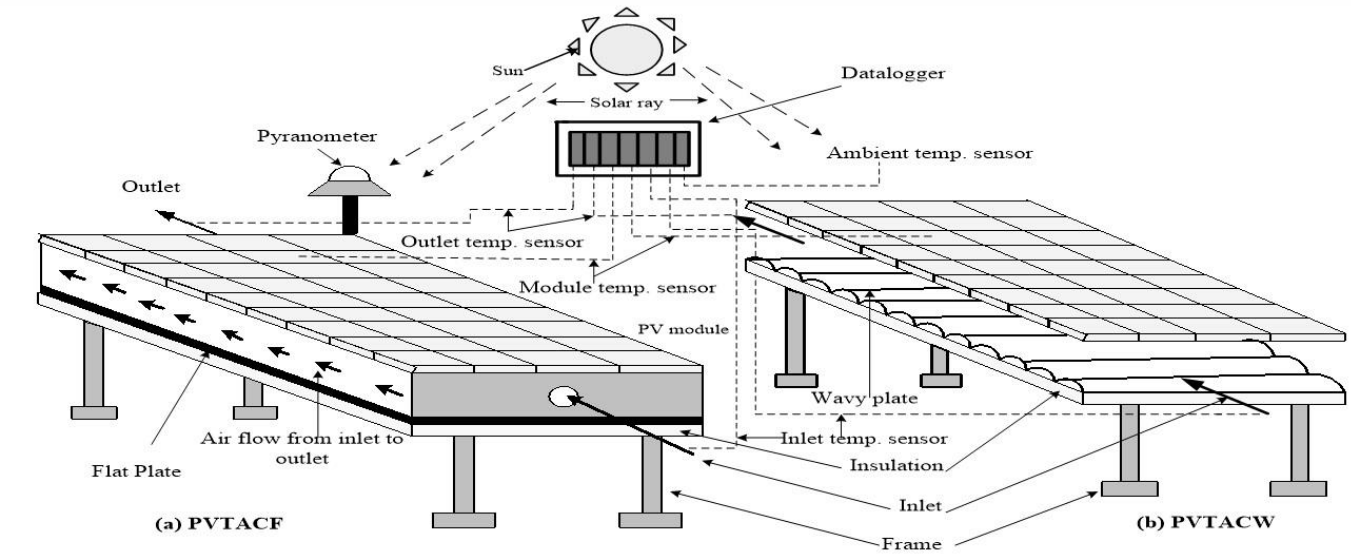
Sun
Solar ray
Datalogger
Pyranometer
Ambient temp. sensor
Outlet
Outlet temp. sensor
Module temp. sensor
PV module
Wavy plate
Air flow from inlet to outlet
Inlet temp. sensor
Insulation
Flat Plate
Inlet
Frame
(a) PVTACF
(b) PVTACW

Fig 1a

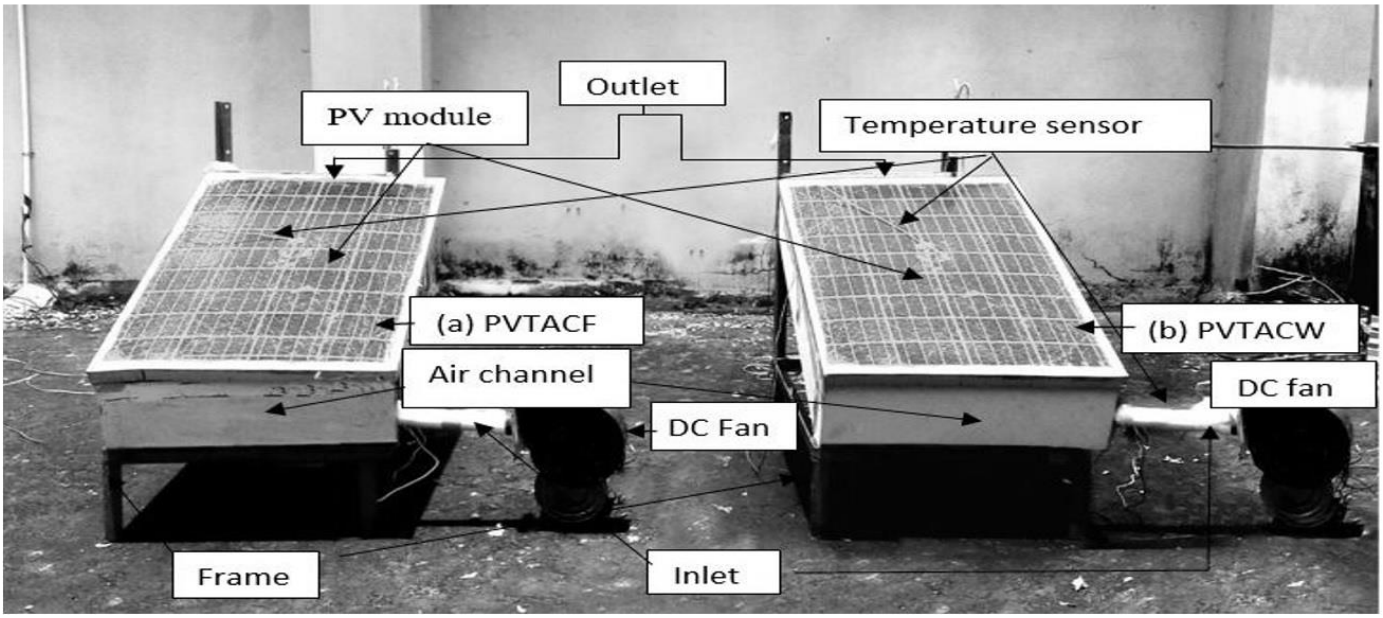
Outlet
PV module
Temperature sensor
(a) PVTACF
(b) PVTACW
Air channel
DC fan
DC Fan
Frame
Inlet

Fig 1b

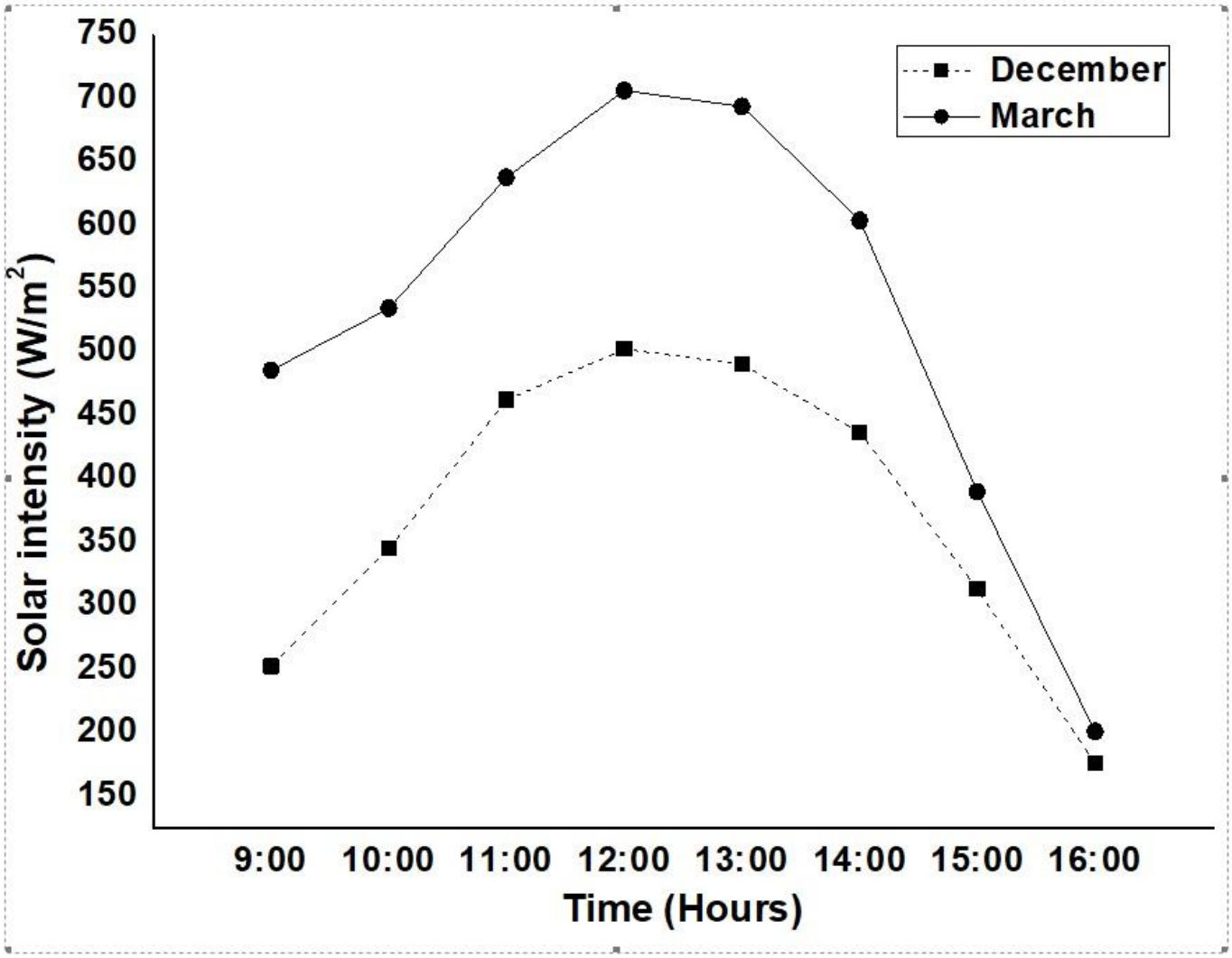
December
March
Solar intensity (W/m^2)
750
700
650
600
550
500
450
400
350
300
250
200
150
9:00
10:00
11:00
12:00
13:00
14:00
15:00
16:00
Time (Hours)

Fig 2.

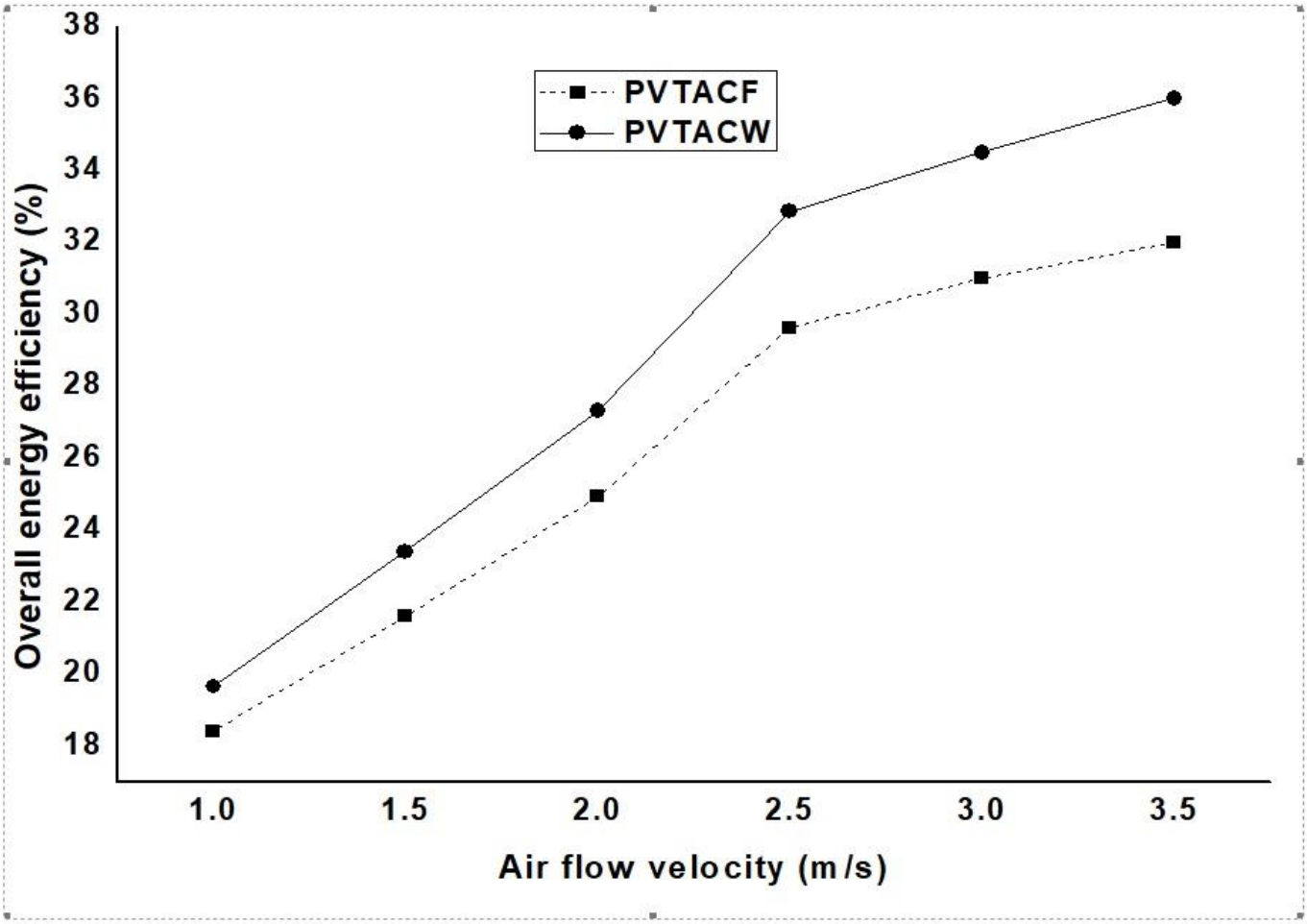
PVTACF
PVTACW
Overall energy efficiency (%)
38
36
34
32
30
28
26
24
22
20
18
1.0
1.5
2.0
2.5
3.0
3.5
Air flow velocity (m/s)

Fig 3.

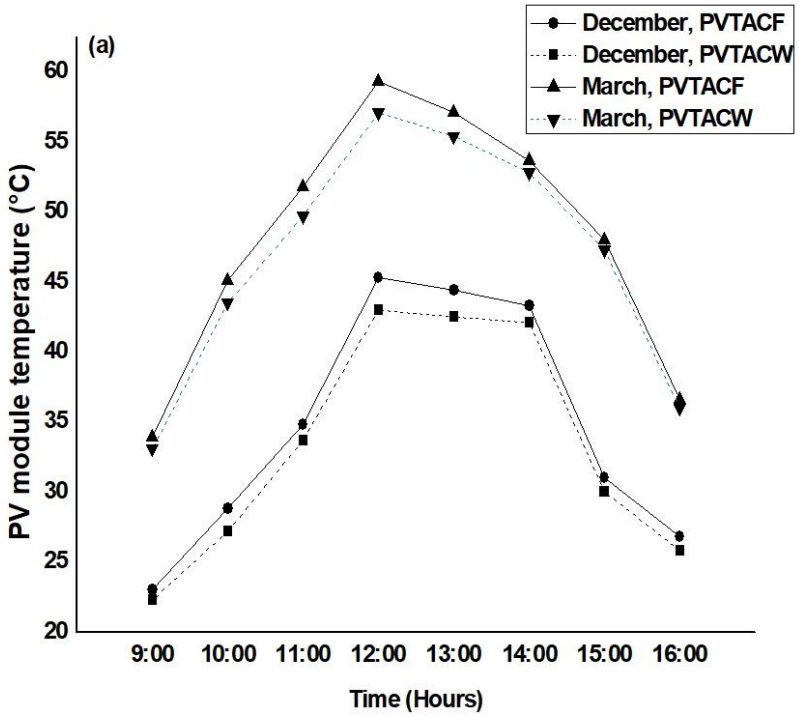
(a)
December, PVTACF
December, PVTACW
March, PVTACF
March, PVTACW
PV module temperature (°C)
60
55
50
45
40
35
30
25
20
9:00
10:00
11:00
12:00
13:00
14:00
15:00
16:00
Time (Hours)

Fig 4a

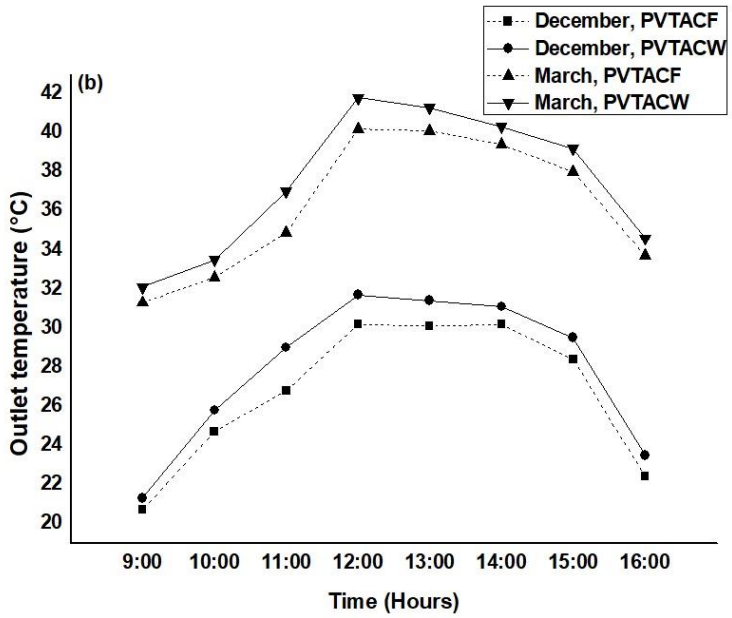
(b)
December, PVTACF
December, PVTACW
March, PVTACF
March, PVTACW
Outlet temperature (°C)
42
40
38
36
34
32
30
28
26
24
22
20
9:00
10:00
11:00
12:00
13:00
14:00
15:00
16:00
Time (Hours)

Fig 4b

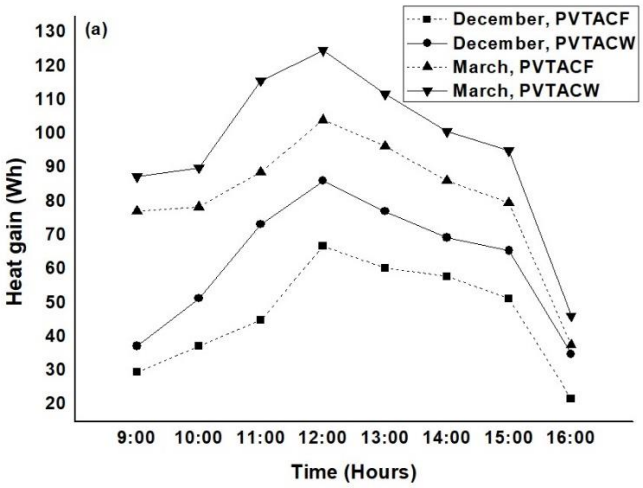

Fig 5a

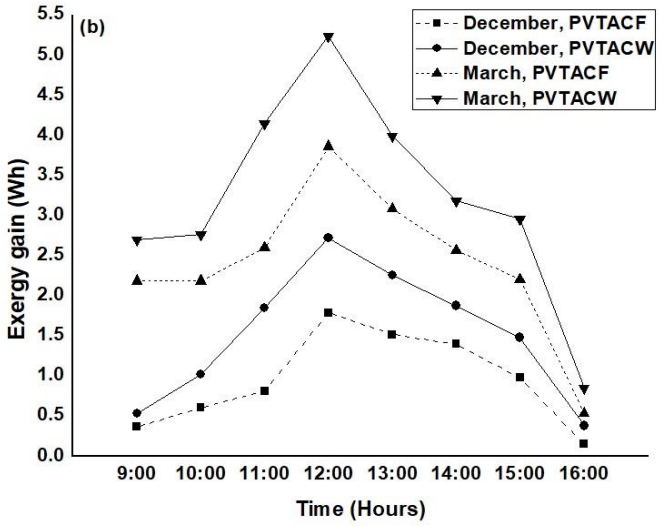

Fig 5b

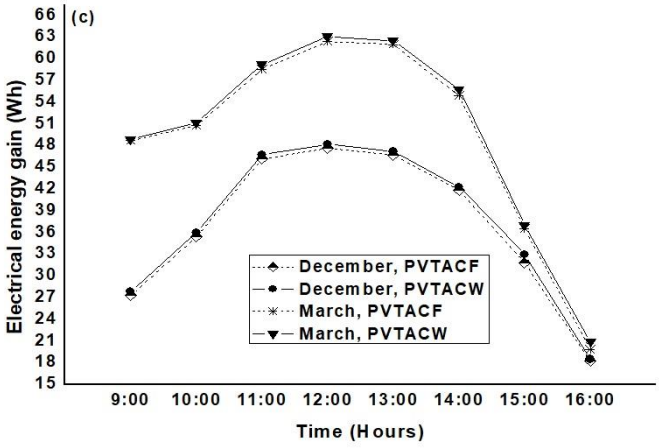

Fig 5c

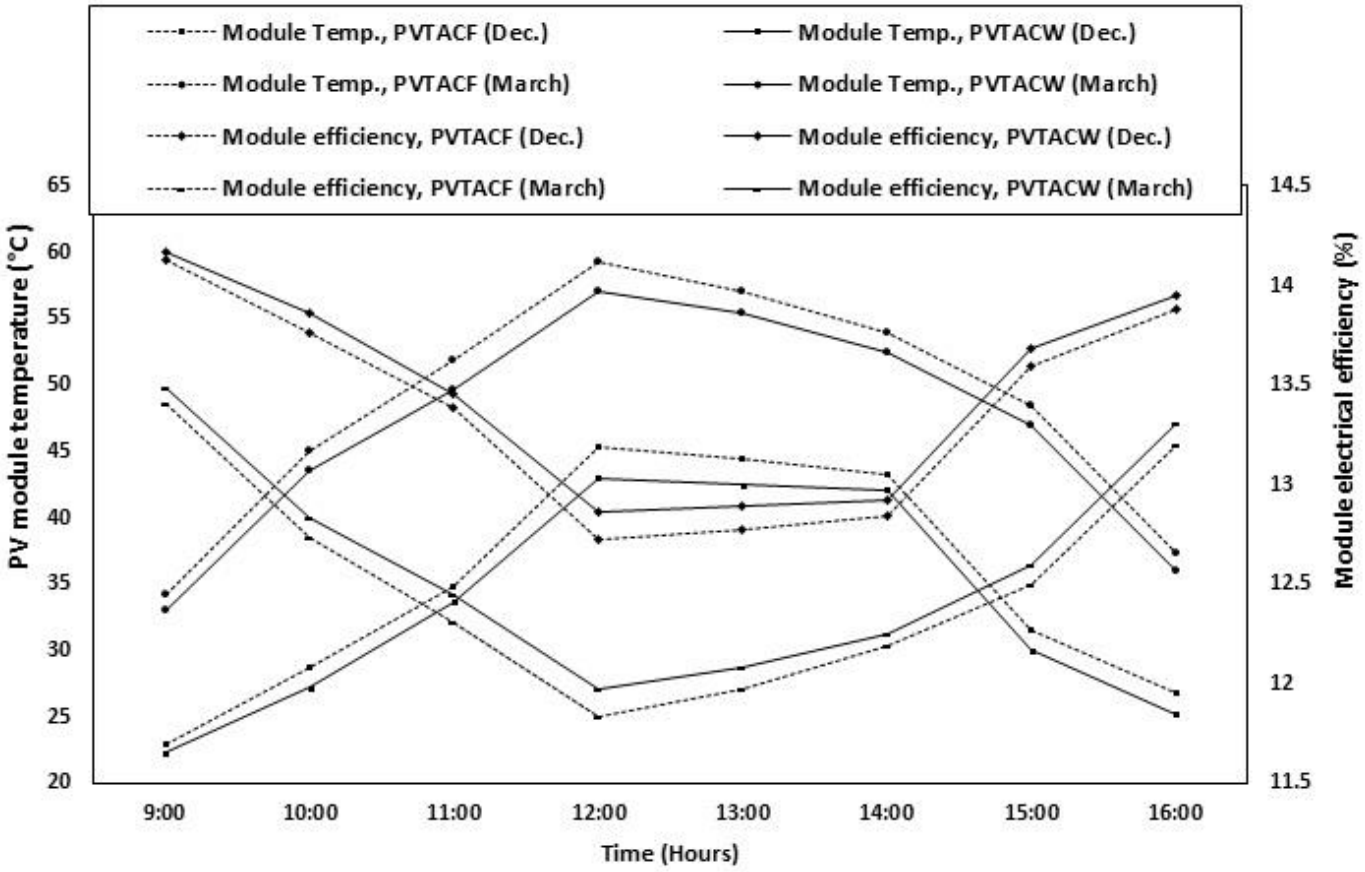
Module Temp., PVTACF (Dec.)
Module Temp., PVTACW (Dec.)
Module Temp., PVTACF (March)
Module Temp., PVTACW (March)
Module efficiency, PVTACF (Dec.)
Module efficiency, PVTACW (Dec.)
Module efficiency, PVTACF (March)
Module efficiency, PVTACW (March)
PV module temperature (°C)
Module electrical efficiency (%)
65
60
55
50
45
40
35
30
25
20
14.5
14
13.5
13
12.5
12
11.5
9:00
10:00
11:00
12:00
13:00
14:00
15:00
16:00
Time (Hours)

Fig 6

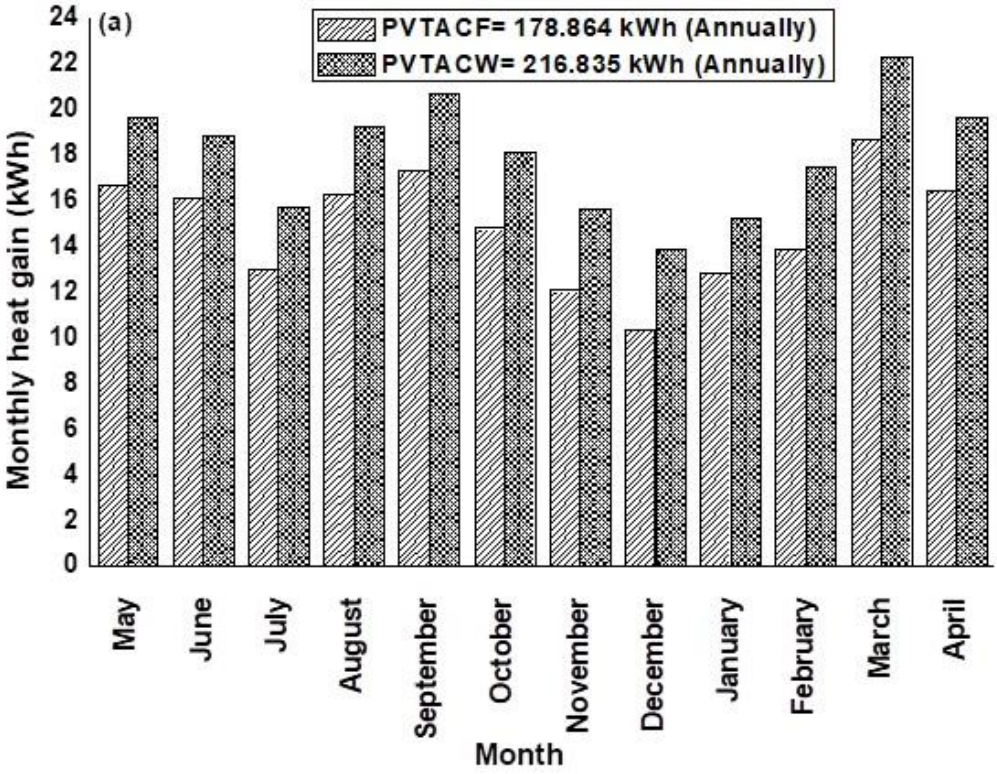
(a)
PVTACF= 178.864 kWh (Annually)
PVTACW= 216.835 kWh (Annually)
Monthly heat gain (kWh)
0
2
4
6
8
10
12
14
16
18
20
22
24
May
June
July
August
September
October
November
December
January
February
March
April
Month

Fig 7a

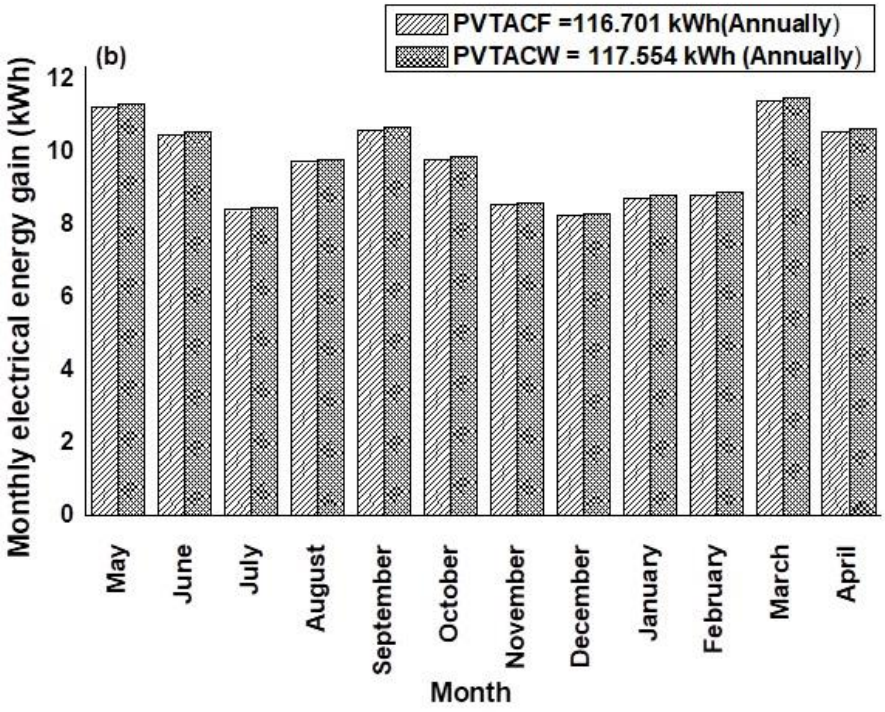
(b)
PVTACF =116.701 kWh(Annually)
PVTACW = 117.554 kWh (Annually)
Monthly electrical energy gain (kWh)
0
2
4
6
8
10
12
May
June
July
August
September
October
November
December
January
February
March
April
Month

Fig 7b

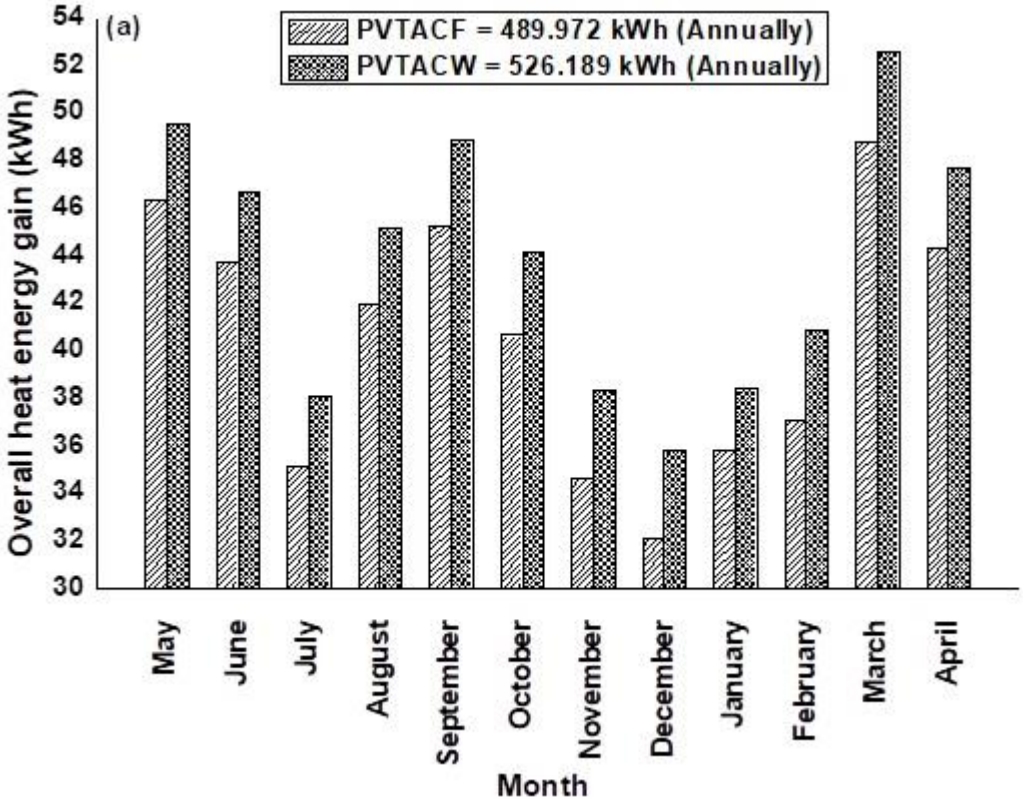
(a)
PVTACF = 489.972 kWh (Annually)
PVTACW = 526.189 kWh (Annually)
Overall heat energy gain (kWh)
54
52
50
48
46
44
42
40
38
36
34
32
30
May
June
July
August
September
October
November
December
January
February
March
April
Month

Fig 8a

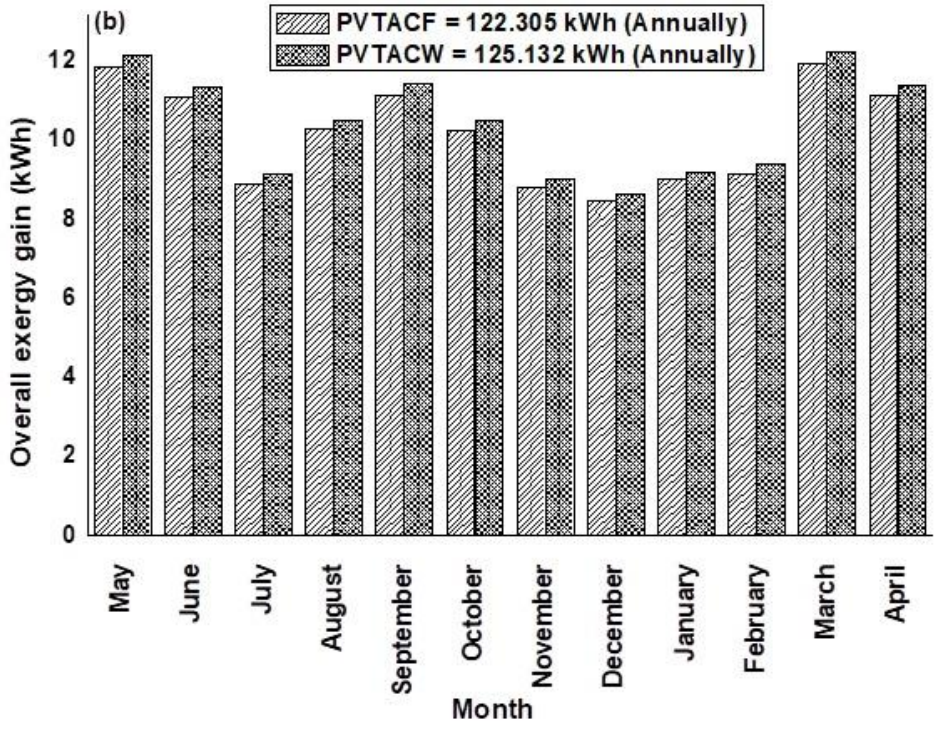
(b)
PVTACF = 122.305 kWh (Annually)
PVTACW = 125.132 kWh (Annually)
Overall exergy gain (kWh)
12
10
8
6
4
2
0
May
June
July
August
September
October
November
December
January
February
March
April
Month

Fig 8b

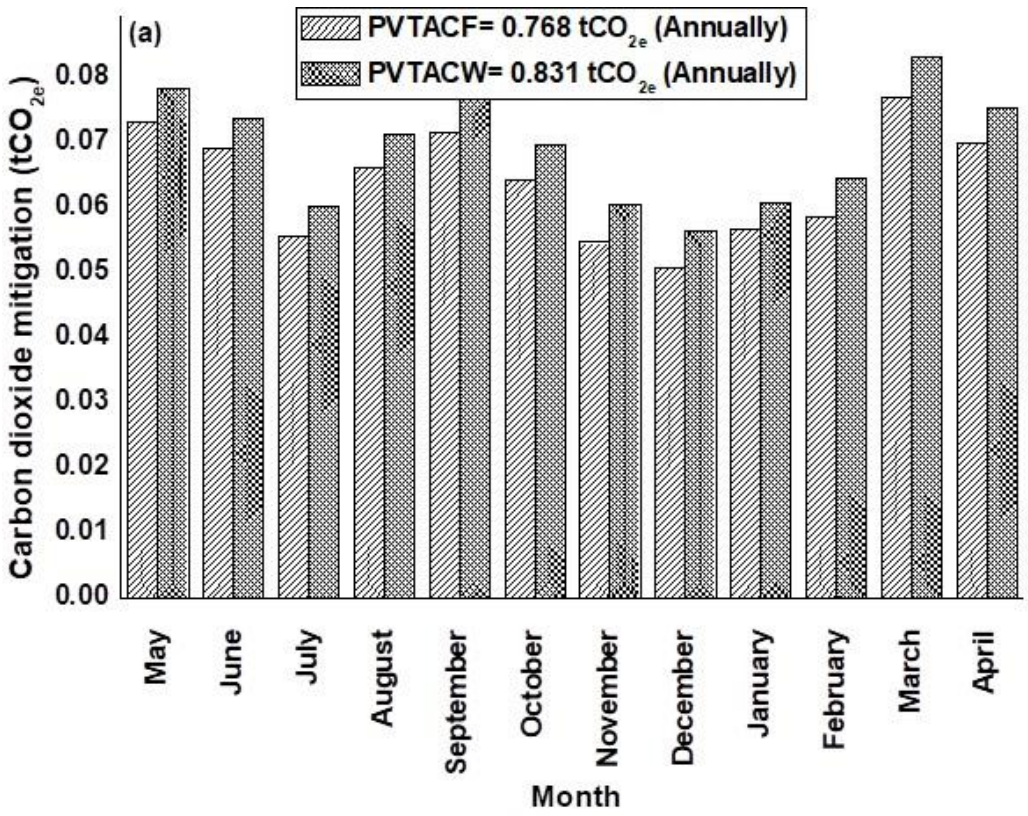
(a)
PVTACF= 0.768 tCO2e (Annually)
PVTACW= 0.831 tCO2e (Annually)
Carbon dioxide mitigation (tCO2e)
0.00
0.01
0.02
0.03
0.04
0.05
0.06
0.07
0.08
May
June
July
August
September
October
November
December
January
February
March
April
Month

Fog 9a

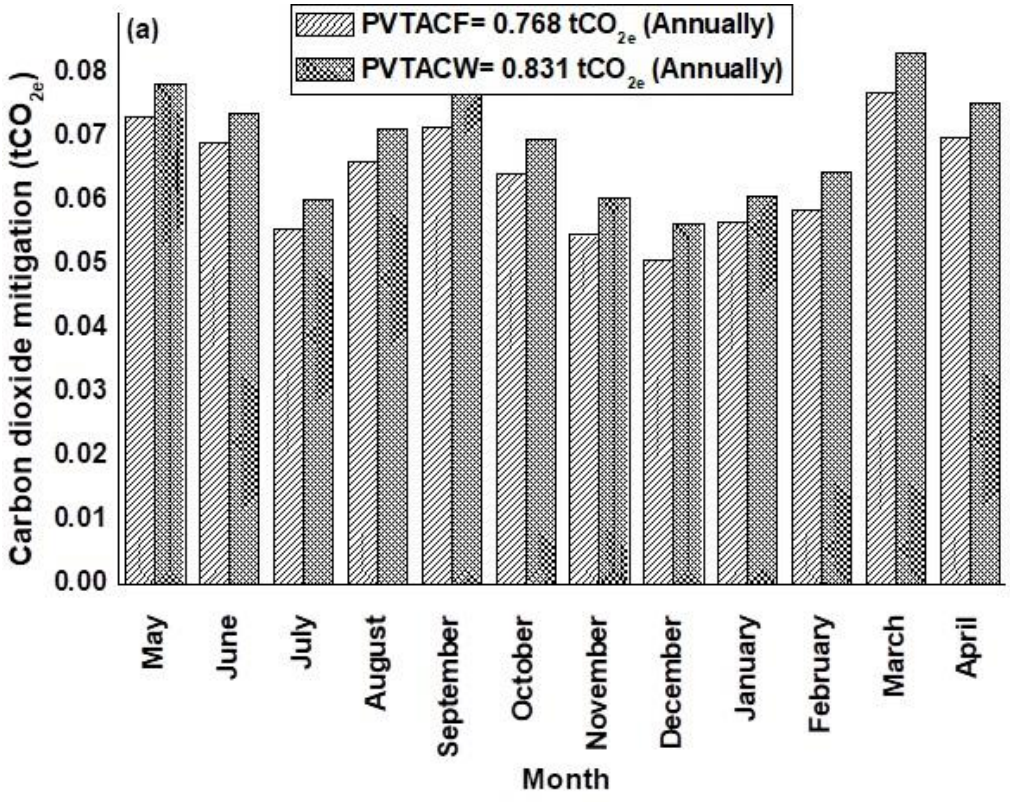
(a)
PVTACF= 0.768 tCO2e (Annually)
PVTACW= 0.831 tCO2e (Annually)
Carbon dioxide mitigation (tCO2e)
0.00
0.01
0.02
0.03
0.04
0.05
0.06
0.07
0.08
May
June
July
August
September
October
November
December
January
February
March
April
Month

Fig 9b